Molecules and Cells

The Bcl-2/Bcl-xL Inhibitor ABT-263 Attenuates Retinal Degeneration by Selectively Inducing Apoptosis in Senescent Retinal Pigment Epithelial Cells

Wonseon Ryu[1,3], Chul-Woo Park[1,3], Junghoon Kim[1], Hyungwoo Lee[1,2], and Hyewon Chung[1,2,*]

[1]Department of Ophthalmology, Konkuk University School of Medicine, Seoul 05029, Korea, [2]Department of Ophthalmology, Konkuk University Medical Center, Seoul 05030, Korea, [3]These authors contributed equally to this work.
*Correspondence: hchung@kuh.ac.kr
https://doi.org/10.14348/molcells.2023.2188
www.molcells.org

Age-related macular degeneration (AMD) is one of the leading causes of blindness in elderly individuals. However, the currently used intravitreal injections of anti-vascular endothelial growth factor are invasive, and repetitive injections are also accompanied by a risk of intraocular infection. The pathogenic mechanism of AMD is still not completely understood, but a multifactorial mechanism that combines genetic predisposition and environmental factors, including cellular senescence, has been suggested. Cellular senescence refers to the accumulation of cells that stop dividing due to the presence of free radicals and DNA damage. Characteristics of senescent cells include nuclear hypertrophy, increased levels of cell cycle inhibitors such as p16 and p21, and resistance to apoptosis. Senolytic drugs remove senescent cells by targeting the main characteristics of these cells. One of the senolytic drugs, ABT-263, which inhibits the antiapoptotic functions of Bcl-2 and Bcl-xL, may be a new treatment for AMD patients because it targets senescent retinal pigment epithelium (RPE) cells. We proved that it selectively kills doxorubicin (Dox)-induced senescent ARPE-19 cells by activating apoptosis. By removing senescent cells, the expression of inflammatory cytokines was reduced, and the proliferation of the remaining cells was increased. When ABT-263 was orally administered to the mouse model of senescent RPE cells induced by Dox, we confirmed that senescent RPE cells were selectively removed and retinal degeneration was alleviated. Therefore, we suggest that ABT-263, which removes senescent RPE cells through its senolytic effect, has the potential to be the first orally administered senolytic drug for the treatment of AMD.

Keywords: ABT-263, Bcl-2/Bcl-xL, doxorubicin, senescence, senolytic

INTRODUCTION

Age-related macular degeneration (AMD) accounts for approximately 10% of cases of blindness worldwide, especially in individuals older than 60 years of age. Researchers have estimated that 288 million people will be diagnosed with AMD worldwide by 2040 (Handa et al., 2019; Wong et al., 2014). AMD is a neurodegenerative disease caused by dysfunction of the retinal pigment epithelium (RPE), photoreceptors, and choroid. The disease is divided into wet and dry AMD. Wet AMD, which affects 10%-20% of patients with AMD, is caused by the growth of choroidal neovascularization. In contrast, dry AMD is distinguished by the accumulation of

Received December 5, 2022; revised January 18, 2023; accepted February 12, 2023; published online May 24, 2023

eISSN: 0219-1032

extracellular deposits called drusen under the RPE (Ding et al., 2009). Dry AMD accounts for approximately 80%-90% of AMD cases, and some patients progress to wet AMD or geographic atrophy, resulting in much more severe vision loss. Currently, the only approved treatment for AMD is an intravitreal injection of anti-vascular endothelial growth factor (VEGF), which suppresses pathological neovascularization (Arepalli and Kaiser, 2021). Repetitive intravitreal injections may lead to serious side effects, such as intraocular infection and retinal detachment (Cox et al., 2021; Falavarjani and Nguyen, 2013).

Although the pathogenesis of AMD is not completely understood, a multifactorial mechanism involving genetic predisposition and environmental factors, including oxidative stress, mitochondrial damage, and cellular senescence, has been suggested (Chen et al., 2010; Kirkland and Tchkonia, 2015; Kozlowski, 2012). Recently, we proved for the first time that the number of senescent RPE cells is increased in mouse models of AMD (both wet and dry) and in old mice compared to young mice, suggesting that RPE senescence might be a new therapeutic target for the treatment of retinal degeneration, including AMD (Chae et al., 2021).

Cellular senescence is induced by various factors, such as telomere erosion, radiation, chemotherapy, oncogene activation, and oxidative stress, resulting in irreversible cell cycle arrest (Di Micco et al., 2021). Senescent cells are not always harmful to tissues; instead, they are necessary during embryonic development and during the wound healing process (Huang et al., 2022). The secretion of cytokines or chemokines from senescent cells, which is called the senescence-associated secretory phenotype (SASP), attracts various immune cells to efficiently remove damaged cells (Birch and Gil, 2020). Furthermore, several growth factors secreted from senescent cells stimulate tissue stem cells or precursor cells to promote tissue regeneration. However, as immune function decreases with age or exposure to continuous cellular stress and senescent cells are not removed in a timely manner, senescent cells accumulate in the tissues, causing chronic inflammation through their SASP and subsequently inducing tissue degeneration (Childs et al., 2015; Lopez-Otin et al., 2013; Serrano and Barzilai, 2018). Therefore, a therapeutic strategy designed to selectively remove senescent cells and prevent tissue degeneration in the context of senescence-related diseases such as AMD is needed.

We recently observed an increased p53 level in senescent RPE cells compared to nonsenescent RPE cells both *in vitro* and *in vivo* and showed that an intravitreal injection of Nutlin-3a, an MDM2 antagonist, selectively eliminates senescent RPE cells through p53-dependent apoptosis, resulting in the alleviation of retinal degeneration (Chae et al., 2021). Another recent report by Crespo-Garcia et al. (2021) showed that the expression of p16 and the antiapoptotic protein Bcl-xL is increased in cells of the vascular unit following oxygen-induced retinopathy in a mouse model. An intravitreal injection of UBX 1967, a Bcl-xL inhibitor, decreases the number of senescent vascular cells and induces the regeneration of blood vessels (Crespo-Garcia et al., 2021).

Among actively studied senolytics, ABT-263, a chemotherapeutic agent developed as an orally administered drug, inhibits the antiapoptotic proteins Bcl-2 and Bcl-xL (Tse et al., 2008). When senescent cells are treated with ABT-263, Bcl-2 is inhibited, and BAX, a proapoptotic protein, is activated (Mohamad Anuar et al., 2020). This drug is being tested in phase 1 and 2 clinical trials for various cancers, and no significant side effects have been reported yet (Rudin et al., 2012; de Vos et al., 2021). A recent study by Chang et al. (2016) also showed that oral administration of ABT-263 results in the selective elimination of senescent bone marrow hematopoietic and muscle stem cells, resulting in the rejuvenation of aged tissue stem cells (Chang et al., 2016). However, the therapeutic potential of this drug has not yet been proven in senescent RPE cells. Thus, in the present study, we investigated the effect of orally administered ABT-263 on senescent RPE cells and sought to determine whether the selective removal of senescent RPE cells ameliorates retinal degeneration.

MATERIALS AND METHODS

Cell culture and treatment

Human retinal pigment epithelial cells (ARPE-19 cells) were purchased from ATCC (#CRL-2302). ARPE-19 cells were cultured in Dulbecco's modified Eagle's medium/F-12 nutrient mixture (DMEM/F-12, #LM 002-04; Welgene, Korea) supplemented with 10% fetal bovine serum (#35-015-CV; Corning, USA), penicillin and streptomycin (#LS202-02; Welgene) in a 37°C incubator with a 5% CO_2 atmosphere. Senescence was induced (Chae et al., 2021) by incubating the cells with 250 nM doxorubicin (Dox, #2252; Tocris Bioscience, UK) for 3 days. Afterward, the medium was changed every 2 days. At 6 days, senescent cells (SnCs) induced by Dox and nonsenescent cells (non-SnCs; maintained in normal growth medium) were treated with vehicle or ABT-263 (ABT, #S1001; Selleckchem, USA) under the indicated conditions.

Experimental animals

Mice were maintained in accordance with the guidelines established by the Konkuk University Institutional Animal Care and Use Committee (IACUC) and housed in a controlled barrier facility within the Konkuk University Laboratory Animal Research Center. All experimental procedures and animal care protocols were approved by the Konkuk University IACUC (KU IACUC; approval No. KU19015) and followed the guidelines provided in the National Institutes of Health Guide for the Care and Use of Laboratory Animals. C57/B6J male mice were obtained from DBL (Korea).

A mixture of Zoletil (Virbac, France) and xylazine (Leverkusen, Germany) (4:1, diluted with normal saline) was administered to anesthetize mice, and the pupils were dilated by applying topical Tropherine eye drops (phenylephrine hydrochloride [5 mg/ml] and tropicamide [5 mg/ml]; Hanmi Pharm, Korea). A mouse model of RPE senescence was established through a subretinal injection of Dox using a previously reported protocol (Chae et al., 2021).

Senescence-associated β-galactosidase (SA-β-gal) staining of ARPE-19 cells and the mouse RPE

A SA-β-gal assay was performed according to the manufac-

turer's protocol (#9860; Cell Signaling Technology, USA). SA-β-gal staining was observed using an inverted microscope (#Axio Scope A1; Carl Zeiss, Germany). The percentage of SA-β-gal-positive cells was quantified. The nuclei were stained with Hoechst 33342 (#H3570; Thermo Fisher Scientific, USA).

Mice were euthanized with CO_2, and eyes were immediately enucleated. After removing the anterior segment, the retina and posterior segment were isolated. Each sample was rinsed with phosphate-buffered saline (PBS), fixed using the provided fixation solution at room temperature for 1 h, and the tissues were stained using the solution provided by the manufacturer for 18 h (#K320; BioVision, USA). Then, the posterior segment was depigmented with 10% H_2O_2 at 55°C for 40 min. The tissues were washed with PBS three times to neutralize H_2O_2. RPE/choroid flat mounts were prepared using sharp forceps and a knife under a microscope (#SZ51; Olympus, Japan).

Cell viability assay

Cell viability was evaluated using the Cell Counting Kit-8 (CCK-8) assay (#CK04; Dojindo, Japan). ARPE-19 cells were seeded in 96-well plates and treated with various concentrations of ABT-263. The conditioned medium was replaced with fresh medium containing 10% CCK-8 reagent, and the cells were incubated for 30 min at 37°C. The absorbance of each well was measured at 450 nm using a SpectraMax ABS Plus instrument (Molecular Devices, USA).

RNA extraction and real-time quantitative PCR

RNA was extracted from ARPE-19 cells using TRIzol (Thermo Fisher Scientific). The cDNA templates were synthesized with a High-Capacity cDNA Reverse Transcription Kit (#4368813; Applied Biosystems, USA) according to the manufacturer's protocol. Relative mRNA expression was assessed using the ΔΔCT method, and the data were normalized to the level of GAPDH. Primers were purchased from Bioneer (Korea) (Table 1).

Immunoblot analysis

Mouse RPE tissues and ARPE-19 cells were lysed with RIPA lysis buffer (Thermo Fisher Scientific) supplemented with a phosphatase and protease inhibitor cocktail (Roche, Switzerland). The protein concentration was measured using the BCA assay (#23227; Pierce, USA), and lysates were separated on an SDS-PAGE gel and transferred to a polyvinylidene difluoride membrane (Millipore, USA). After blocking with 5% nonfat milk in TBS supplemented with 0.05% Tween 20 (TBS-T) for 1 h, the membranes were incubated at 4°C overnight with primary antibodies against Bcl-2 (#sc-7382; Santa Cruz Biotechnology, USA), Bcl-xL (#sc-8392; Santa Cruz Biotechnology), BAX (#20067; Santa Cruz Biotechnology), caspase-9 (#9508S; Cell Signaling Technology), caspase-3 (#9662S; Cell Signaling Technology), p53 (#sc-126; Santa Cruz Biotechnology), p21 (#sc-6246; Santa Cruz Biotechnology), p16 (#51-1325GR; BD Pharmingen, USA), and β-actin (#sc-20067; Santa Cruz Biotechnology). The membranes were washed with TBS-T and incubated with HRP-conjugated anti-mouse (#7076S; Cell Signaling Technology) or anti-rabbit (#7074S; Cell Signaling Technology) antibodies in the blocking solution for 1 h. Protein expression levels were determined using ECL reagents (Thermo Fisher Scientific) and a ChemiDoc instrument (#CL-1000; Thermo Fisher Scientific) and quantified with ImageJ software (NIH). β-Actin served as a loading control.

Immunofluorescence staining and BrdU assay

ARPE-19 cells were treated with 10 μM BrdU (#B5002; Sigma-Aldrich, USA). Then, the cells were fixed with 4% paraformaldehyde for 30 min and permeabilized with PBS containing 0.1% Triton X-100 (PBS-T) for 15 min. The cells were treated with 2 N HCl at 37°C for 30 min for denaturation and washed twice with 0.1 M borate buffer for neutralization. Mouse RPE tissues or ARPE-19 cells were blocked with 3% BSA in PBS-T (blocking solution) for 1 h and incubated with anti-BrdU (#MA3-071; Invitrogen, USA), anti-ZO-1 (#61-7300; Invitrogen), anti-cleaved caspase-3 (#9661; Cell Signaling Technology), anti-lamin A/C (LMNA, #sc-376248; Santa Cruz Biotechnology), anti-p53, anti-p21, anti-p16 (#sc-1661; Santa Cruz Biotechnology), or anti-Ki67 (#ab15580; Abcam, UK) antibodies in blocking solution at 4°C overnight. The samples were washed with PBS, and a fluorescent dye-conjugated secondary antibody (#A-11029, #A-21424, #A-21429, #A-11034; Thermo Fisher Scientific) was applied and

Table 1. Primer list

Gene	Forward sequence	Reverse sequence
Bcl-2	GAACTGGGGGAGGATTGTGG	CCGTACAGTTCCACAAAGGC
Bcl-xL	GCTTGGATGGCCACTTACCT	CGACTGAAGAGTGAGCCCAG
BAX	GAACCATCATGGGCTGGACA	GCGTCCCAAAGTAGGAGAGG
BAK	CAGGAACAGGAGGCTGAAGG	ATAGGCATTCTCTGCCGTGG
BIM	CAAGAGTTGCGGCGTATTGG	ACCAGGCGGACAATGTAACG
P53	TGGCCATCTACAAGCAGTCA	GGTACAGTCAGAGCCAACCT
P21	GATGAGTTGGGAGGAGGCAG	CGGCGTTTGGAGTGGTAGAA
P16	GAGCAGCATGGAGCCTTC	TAACTATTCGGTGCGTTGGG
TNF-α	TCTTCTCGAACCCCGAGTGA	TATCTCTCAGCTCCACGCCA
TNF-β	CATGTGCCTCTCCTCAGCTC	GTGTGGGTGGATAGCTGGTC
MMP2	TGGCAAGTACGGCTTCTGTC	TTCTTGTCGCGGTCGTAGTC
MMP9	GCAATGCTGATGGGAAACCC	AGAAGCCGAAGAGCTTGTCC

incubated for 2 h. Afterward, the samples were treated with Hoechst 33342 (#H3570; Invitrogen) in PBS for 15 min to stain the nuclei. The samples were mounted with Aqua-Poly/Mount (#18696-20; Polysciences, USA). Images were captured with a confocal microscope (#LSM 900; Carl Zeiss).

EdU labeling and FACS analysis

For the determination of the cellular proliferation rate, ARPE-19 cells were labeled with EdU and analyzed according to the manufacturer's protocol (#C10337; Invitrogen). Briefly, ARPE-19 cells were incubated with 10 μM EdU for 2 h, followed by cell detachment. The detached cells were fixed with 4% PFA for 15 min, permeabilized with 0.5% Triton X-100 for 20 min at room temperature and incubated with Click-iT® reaction cocktails for 30 min. The EdU-labeled ARPE-19 cells were analyzed using a CytoFLEX instrument (Beckman Coulter, USA).

H&E staining

Immediately after enucleation, the eyes were placed in embedding molds filled with optimal cutting temperature compound (#FSC 22; Leica, Germany) and placed on dry ice. Then, the frozen samples were serially sectioned at a 10-μm thickness using a cryostat (#CM1860; Leica) and stained with H&E. The retinal outer nuclear layer (ONL) thickness was measured, and then the values were averaged.

Color fundus photography and fundus autofluorescence imaging

Color fundus photos and fundus autofluorescence images were obtained using a fundus camera (#TRC-50 IX; Topcon, Japan) after mydriasis using Tropherine eye drops (Hanmi Pharm). Digital images were captured with a camera (Nikon, Japan).

Electroretinography

Retinal function was assessed *in vivo* by performing electroretinography (ERG). ERG recordings were obtained using a Celeris rodent ERG system (Diagnosys, USA). The mice were dark-adapted for at least 16 h overnight prior to the experiment. The mice were anesthetized, the pupils were dilated, 2% hypromellose (Samil, Korea) was applied, and an electrode was inserted. For ERG, a platinum needle was injected into the subcutaneous area in the middle of the forehead, and a grounding electrode was placed in the caudal area. Scotopic ERG responses were stimulated by a single-flash stimulus. For each flash intensity, a minimum of three responses were recorded and averaged. The amplitudes of a- and b-waves were assessed from the maximal negative and positive recordings with respect to the baseline before stimulation.

Statistical analysis

All sets of experiments were repeated at least three times. The data are presented as the mean ± SD. The significance of differences between the control and experimental groups was determined using an unpaired two-tailed Student's *t*-test, and multiple datasets were compared using one-way ANOVA followed by Fisher's least significant difference post hoc test or Tukey's multiple comparisons tests ($*P < 0.05$, $**P < 0.01$, and $***P < 0.001$) with Prism 5 software (GraphPad Software, USA).

RESULTS

Selective elimination of senescent RPE cells by ABT-263 *in vitro*

We induced ARPE-19 cell senescence with Dox to investigate the senolytic effect of ABT-263. As described in our previous study (Chae et al., 2021), ARPE-19 cell senescence was induced by treatment with 250 nM Dox for 3 days, the culture medium containing Dox was refreshed daily, and the Dox-treated cells were cultured for another 4 days. Dox-induced SnCs were treated with various concentrations of ABT-263 for 24 h and stained with SA-β-gal (Fig. 1A). ABT-263 reduced the number of SA-β-gal-positive SnCs in a concentration-dependent manner. Treatment with 1.25 μM ABT-263 reduced the number of SA-β-gal-positive cells among SnCs by 64.9% (Fig. 1B). Moreover, 1.25 μM ABT-263 reduced the viability of SnCs to 65.2%, but the viability of non-SnCs was not affected (Fig. 1C), suggesting that 1.25 μM ABT-263 selectively removed SnCs.

Apoptosis of senescent RPE cells induced by ABT-263 *in vitro*

We hypothesized that ABT-263 selectively induces the apoptosis of senescent cells by targeting the antiapoptotic proteins Bcl-2 and Bcl-xL. First, the protein and mRNA levels of Bcl-2 family proteins were investigated after treatment with 1.25 μM ABT-263. Interestingly, the level of the Bcl-2 protein was significantly decreased in SnCs treated with ABT-263. However, as the level of the proapoptotic protein BAX was not altered by ABT-263 treatment, we measured the ratio of BAX/Bcl-2 as a marker of apoptosis. The BAX/Bcl-2 ratio was significantly increased in SnCs treated with ABT-263, which resulted from reduced levels of Bcl-2 (Fig. 2A). Since the SnCs were selectively eliminated by the ABT-263 treatment, the mRNA levels of proapoptotic Bcl-2 family proteins (BAX, BAK, and BIM) were significantly decreased in the SnCs treated with 1.25 μM ABT-263 (Fig. 2B). Then, to confirm whether the reduced viability of SnCs following ABT-263 treatment resulted from apoptosis, we investigated the levels of the active caspase-3 and -9 proteins (cleaved caspase-3 and -9; CC3 and CC9) in SnCs treated with ABT-263 at various time points. Levels of the CC3 and CC9 proteins increased up to 3 h, decreased after 6 h, and returned to the baseline level at 24 h (Fig. 2C). Then, the expression of p53, a marker of cellular senescence, and LMNA was investigated. LMNA is used to visualize the shape of the nucleus since it forms the internal nuclear membrane structure (Dubik and Mai, 2020). In the non-SnCs and the non-SnCs treated with ABT-263, p53 and CC3 were expressed at very low levels, as determined by immunofluorescence staining. However, the level of p53 was markedly increased in SnCs, and a micronuclei phenotype was observed; however, CC3 was not detected. When SnCs were treated with ABT-263, approximately 44.2% of the cells were positive for CC3. In addition, the colocalization of CC3 with p53 or LMNA in SnCs treated with ABT-263 further indicated the selective elimination of SnCs by apoptosis (Fig.

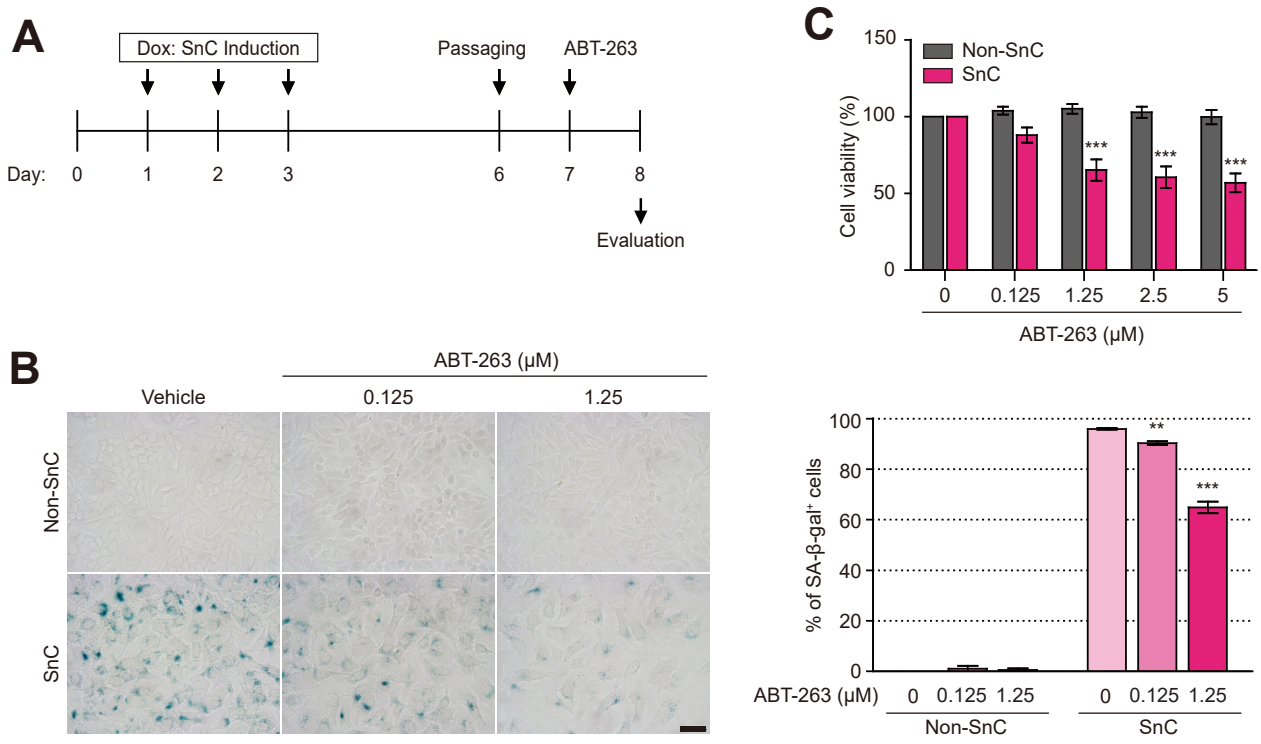

Fig. 1. ABT-263 selectively kills Dox-induced senescent retinal pigment epithelium (RPE) cells. (A) Schematic of the ARPE-19 cell experiments shown in (B and C). ARPE-19 cells were cultured in normal medium containing 250 nM doxorubicin (Dox) for 3 days to obtain senescent ARPE-19 cells (SnCs), and then the medium was replaced with fresh medium every 2 days. After 7 days, the cells were treated with ABT-263 (0, 0.125, 1.25, 2.5, or 5 μM) for 24 h. (B) Senescence-associated β-galactosidase (SA-β-gal) staining of nonsenescent cells (non-SnCs) and SnCs treated with 0, 0.125, or 1.25 μM ABT-263 for 24 h. The graph shows the percentage of SA-β-gal-positive cells among non-SnCs and SnCs. Scale bar = 50 μm. (C) Viability of non-SnCs and SnCs after treatment with various concentrations of ABT-263 for 24 h (n = 5). The data are presented as the mean ± SD. $^{**}P < 0.01$ and $^{***}P < 0.001$ according to ANOVA.

2D). Collectively, these results suggest that ABT-263 selectively killed SnCs by inducing apoptosis.

An ABT-263-induced decrease in the expression of markers of cellular senescence *in vitro*

Next, the expression of markers of cellular senescence and SASP components was investigated upon treatment with ABT-263. The increased expression of the p53, p21, and p16 mRNAs (Kim and Kim, 2021; Lee, 2022) or proteins in SnCs compared to non-SnCs was significantly decreased by the ABT-263 treatment (Fig. 3A). The increase in the levels of SASP components, including TNF-α, TNF-β, MMP-2, and MMP-9, in SnCs compared to non-SnCs was also significantly decreased (Fig. 3B). The number of BrdU- and EdU-positive cells was significantly increased in the SnCs treated with ABT-263 compared to the SnCs treated with vehicle, suggesting that the proliferative capacity of the remaining nonsenescent cells was at least partially recovered due to the improvement in the microenvironment resulting from the selective removal of senescent cells (Fig. 3C).

Alleviation of retinal degeneration by ABT-263 in a mouse model of RPE senescence

Since ABT-263 selectively kills senescent RPE cells *in vitro*, we investigated whether ABT-263 alleviates retinal degeneration by exerting a senolytic effect on senescent RPE cells *in vivo*. As described in our previous study, Dox (100 ng/μl) was injected into the subretinal space of mice, and cellular senescence in the RPE was assessed by performing SA-β-gal staining of RPE/choroid flat mounts obtained at 3, 7, and 14 days (Chae et al., 2021). The level of SA-β-gal staining in the RPE/choroid flat mounts peaked at 7 days after the Dox injection and was significantly decreased at 14 days. Thus, in this experiment, RPE cell senescence was induced by subretinal injections of Dox (100 ng/μl) for 7 days. The three experimental groups were mice that were subretinally injected with vehicle and orally administered vehicle for 7 days (control), mice subretinally injected with Dox and orally administered vehicle for 7 days (Dox), and mice subretinally injected with Dox and orally administered 50 mg/kg ABT-263 for 7 days (DA) (Fig. 4A). Body weight was measured daily for 7 days, and no difference in body weight was observed among the three groups (Fig. 4B). The mice in each group showed appropriate locomotor abilities (data not shown). The atrophic area, which indicates retinal degeneration, in the color fundus photos was reduced by 48.5% in the DA group compared to the Dox group. In addition, the area of autofluorescence (AF), which is associated with lipofuscin accumulation,

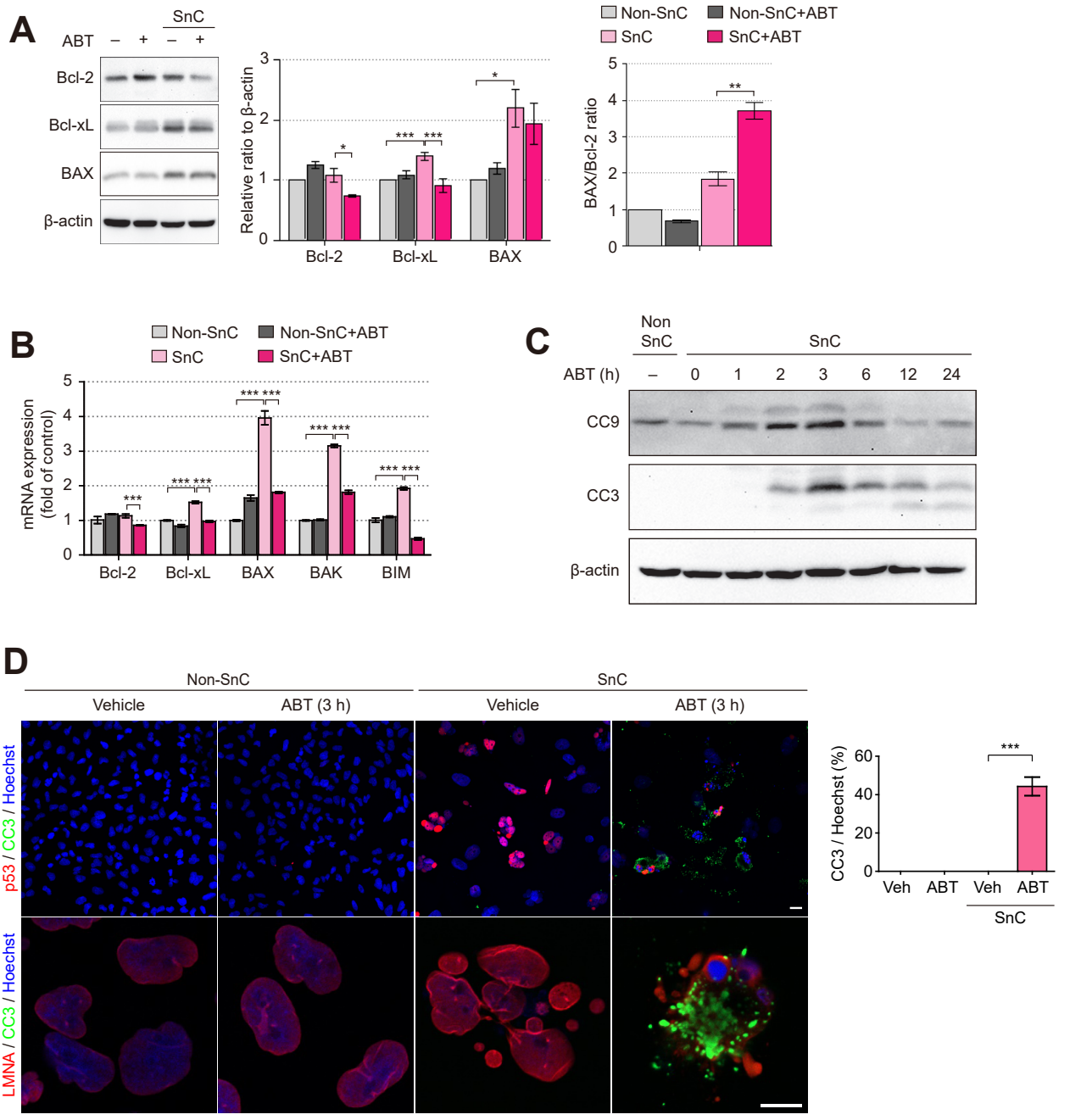

Fig. 2. ABT-263 induces apoptotic death of senescent RPE cells. (A) Immunoblots showing Bcl-2, Bcl-xL, and BAX levels in non-SnCs and SnCs exposed to 1.25 μM ABT-263 for 24 h. β-Actin was used as a loading control. Densitometric quantification of Bcl-2 and BAX was performed, and the BAX/Bcl-2 ratio (right panel) was calculated. (B) The mRNA expression levels of *Bcl-2*, *Bcl-xL*, *BAX*, *BAK* and *BIM* in non-SnCs and SnCs treated with 1.25 μM ABT-263 for 24 h. (C) Immunoblots showing the levels of cleaved caspase-9 (CC9) and cleaved caspase-3 (CC3). Non-SnCs and SnCs were treated with 1.25 μM ABT-263 for various durations. β-Actin was used as a loading control. (D) Representative images showing the immunofluorescence staining of non-SnCs and SnCs that had been treated with ABT-263 for 3 h. The cells were stained with anti-CC3 (green), anti-p53 (red), or anti-lamin A/C (LMNA; red) antibodies. The nuclei were stained with Hoechst (blue). The graph shows the percentage of cells costained with Hoechst and CC3. Scale bars = 20 μm. The data are representative of three experiments and are presented as the mean ± SD. $*P < 0.05$, $**P < 0.01$, and $***P < 0.001$ according to ANOVA.

was reduced in the DA group compared to the Dox group (Fig. 4C). Similarly, the SA-β-gal-positive area in RPE flat mounts was reduced by 40.2% in the DA group compared to the Dox group. Prominent SA-β-gal staining was observed in the RPE layer in cryosectioned retinas from the Dox group, and SA-β-gal staining was reduced in the DA group. The ONL

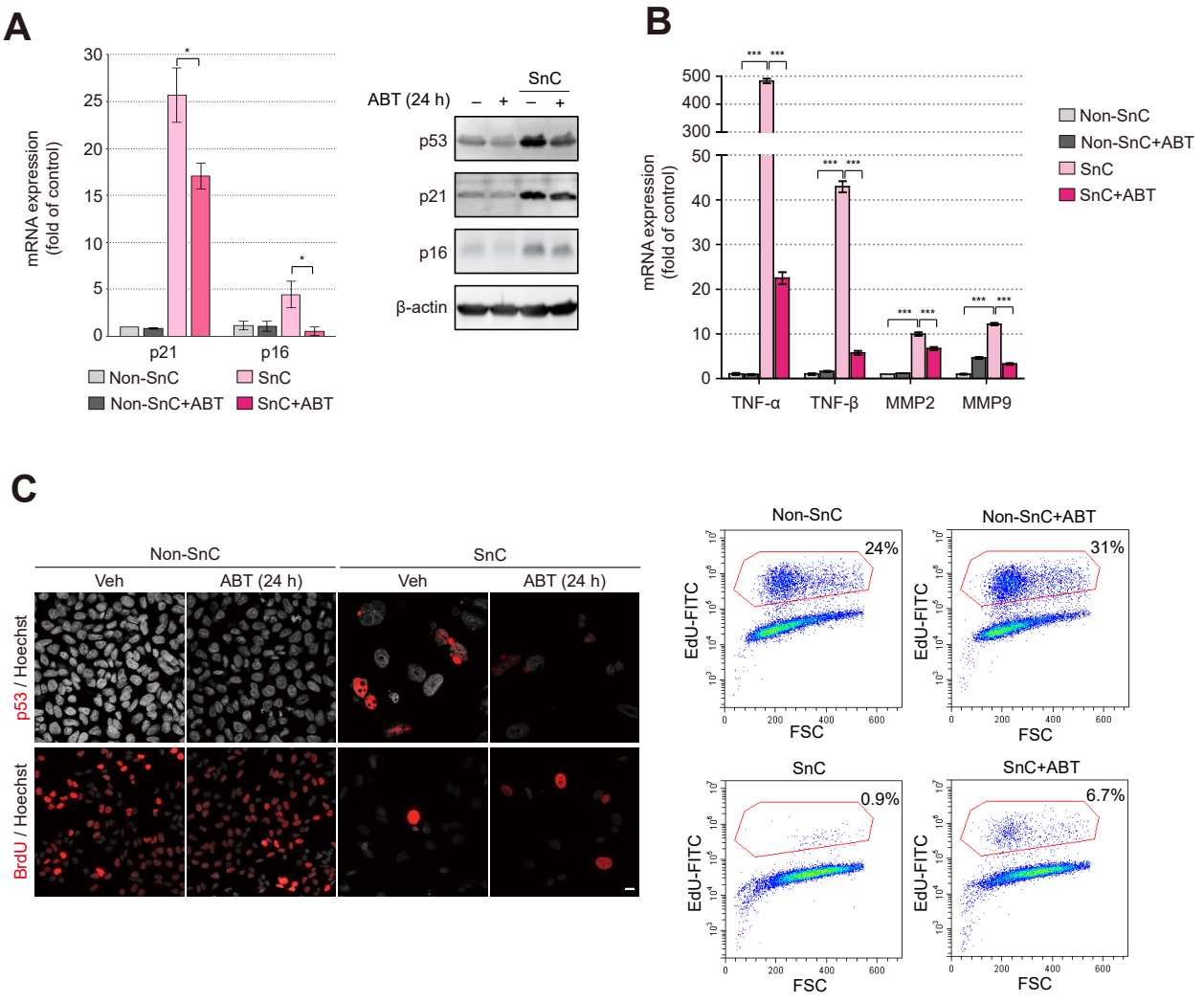

Fig. 3. ABT-263 reduces the levels of senescence markers induced by Dox treatment. (A) The levels of senescence markers in non-SnCs and SnCs treated with 1.25 μM ABT-263 for 24 h. The senescence markers were confirmed by measuring mRNA expression (left panel) and protein levels (right panel). (B) The mRNA expression of SASP factors (*TNF-α*, *TNF-β*, *MMP2*, and *MMP9*) in non-SnCs and SnCs treated with 1.25 μM ABT-263 for 24 h. *GAPDH* served as a housekeeping gene. (C) Immunofluorescence staining and analysis of the expression of p53 and BrdU incorporation (left panel) (p53 and BrdU, red; Hoechst, dark gray). Mass cytometry plot of cells that were stained with EdU and Click-iT® reaction cocktails (right panel). Scale bar = 20 μm. The data are presented as the mean ± SD. $*P < 0.05$ and $***P < 0.001$ according to ANOVA.

thickness was increased by 10% in the DA group compared to the Dox group (Fig. 4D).

Immunofluorescence staining showed that the expression of p53, p21, and p16 was increased in the RPE flat mounts from the Dox group compared to the control group and was decreased in the DA group. In addition, the level of Ki67 in the DA group was increased compared to that in the Dox group, suggesting a partial restoration of RPE cell proliferation (Fig. 4E). Levels of Bcl-xL, p21 and p16 proteins were also decreased in the mouse RPE upon ABT-263 treatment (Fig. 4F). We performed ERG to confirm that ABT-263 treatment improves visual function. The dark-adapted response waveforms of mice from the DA group showed a significant recovery of a- and b-wave amplitudes (Fig. 4G), indicating that the selective removal of senescent cells induced by the oral administration of ABT-263 improved visual function.

DISCUSSION

Currently, anti-VEGF agents are the only approved treatments for wet (neovascular) AMD; however, anti-VEGF agents have limited therapeutic effects and require repeated administration (Comparison of Age-related Macular Degeneration Treatments Trials (CATT) Research Group et al., 2016). Moreover, an U.S. Food and Drug Administration (FDA)-approved treatment is not available for dry AMD (Cabral de Guimaraes et al., 2022). Therefore, new strategies for the treatment of both wet and dry AMD are needed. Our recent study con-

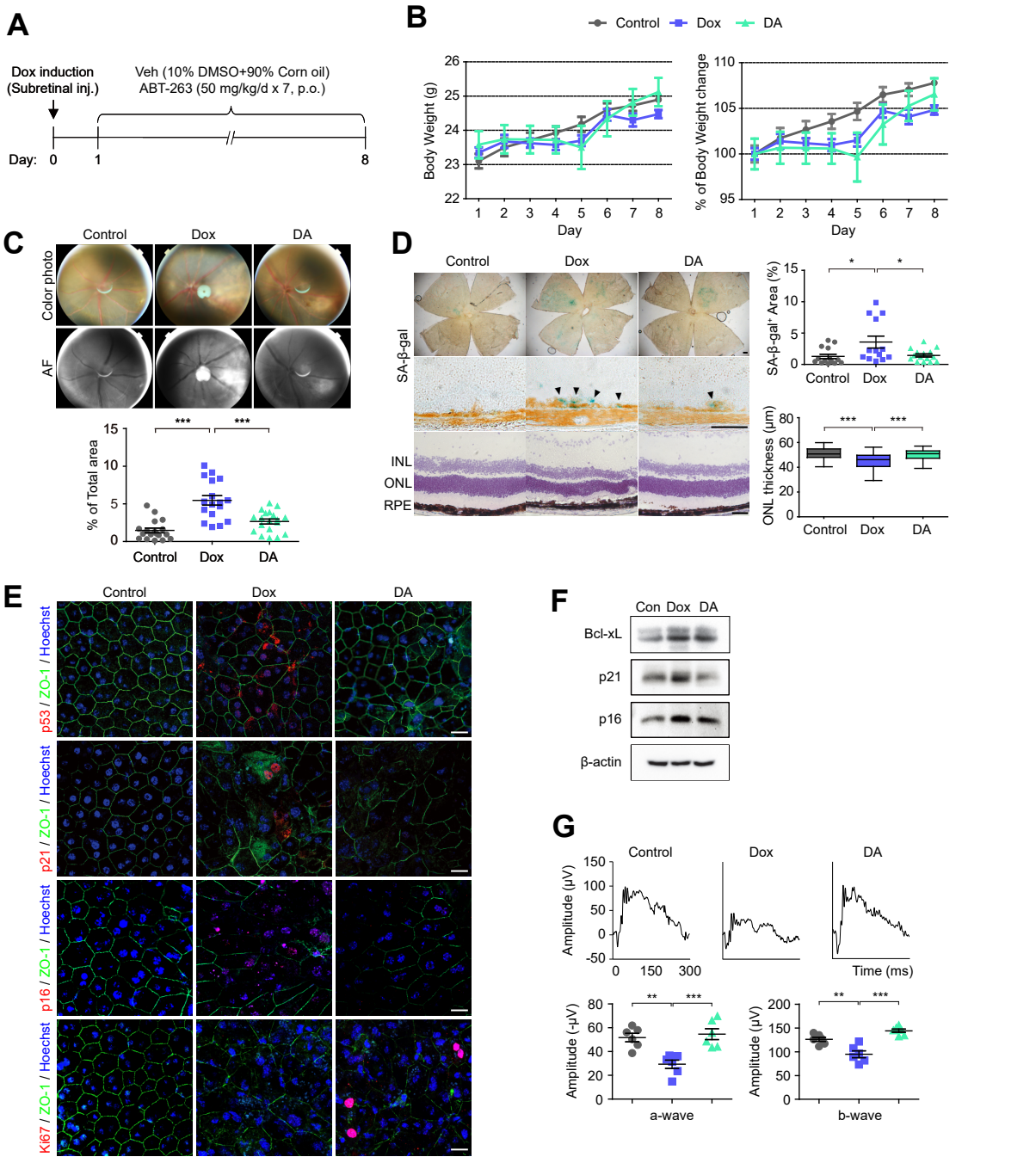

Fig. 4. ABT-263 ameliorates retinal degeneration induced by RPE senescence. (A) Schematic of the time course experiments shown in (B-G). The three experimental groups were mice that were subretinally injected (Subretinal inj.) with vehicle (Veh) and orally administered (p.o.) vehicle for 7 days (control), mice subretinally injected with Dox and orally administered vehicle for 7 days (Dox), and mice subretinally injected with Dox and orally administered 50 mg/kg ABT-263 for 7 days (DA). (B) Changes in body weight during the experiments (n = 4). (C) Color fundus photos and autofluorescence images of the three groups. The graph shows the percentage of the atrophic area relative to the total autofluorescence (AF) area. (D) Representative images of SA-β-gal staining of RPE flat mounts and sectioned retinas (arrowheads) and H&E staining of sectioned retinas from the three groups (INL; inner nuclear layer, ONL; outer nuclear layer, RPE; retinal pigment epithelium). The graphs show the percentages of SA-β-gal-positive area (upper panel) and ONL thickness (lower panel) (n = 3). Scale bars = 50 μm. (E) Images showing immunofluorescence staining for p53, p21, p16, and Ki67 (red) in the three groups. The nuclei were stained with Hoechst (blue). Scale bars = 20 μm. (F) Immunoblots showing the levels of Bcl-xL, p21 and p16 in RPE cells from the three groups. (G) Electroretinography (ERG) results for the control, Dox, and DA groups. The mean amplitude was significantly restored in the DA group compared to the Dox group (n = 6). The data are presented as the mean ± SD. $*P < 0.05$, $** P < 0.01$, and $***P < 0.001$ according to ANOVA.

firmed the presence of senescent RPE cells in mouse models of AMD and aged mice. Upon the intravitreal administration of the senolytic drug Nutlin-3a, retinal function was improved via the selective removal of senescent RPE cells (Chae et al., 2021). Another recent study by Crespo-Garcia et al. (2021) reported the presence of senescent retinal endothelial cells in a mouse model of ischemic retinopathy. The researchers showed the increased expression of the senescence marker p16INK4A and the proapoptotic protein Bcl-xL in a mouse model of ischemic retinopathy and found that the Bcl-xL inhibitor UBX 1967 removes senescent endothelial cells, ameliorating ischemic retinopathy (Crespo-Garcia et al., 2021).

In the present study, we investigated whether senescent RPE cells showed increased expression of the proapoptotic proteins Bcl-2 and Bcl-xL and were selectively eliminated by ABT-263, a known Bcl-2 and Bcl-xL inhibitor. First, we confirmed that the viability of senescent ARPE-19 cells was decreased after treatment with ABT-263 at concentrations ranging from 1.25-2.5 μM through the induction of apoptosis, whereas the viability of nonsenescent ARPE-19 cells remained unchanged. The expression of markers of cellular senescence, including p53, p21 and p16, and SASP factors, such as TNF-α, TNF-β, MMP2, and MMP9, was reduced upon the elimination of senescent ARPE-19 cells.

Regarding the possibility that ABT-263 could be used as an oral drug for AMD, other Bcl-2 inhibitors have already been tested in clinical trials. Oblimersen, which inhibits Bcl-2 mRNA expression through hybridization using a short 18-mer RNA, was assessed in a phase 1 trial, and venetoclax, which targets BH3-binding sites on Bcl-2, was shown to ameliorate chronic lymphocytic leukemia and was approved by the FDA. Obatoclax mesylate, a BH3 mimetic, binds most Bcl-2 family members and is currently being studied in phase 2 clinical trials (Han et al., 2019). ABT-263 was recently assessed in phase 1 clinical trials as a treatment for malignancies, including small-cell lung cancer and chronic lymphoid leukemia. In addition, phase 2 clinical trials of its effects on these diseases are ongoing (Gandhi et al., 2011; Kipps et al., 2015; Rudin et al., 2012; de Vos et al., 2021; Wilson et al., 2007). Although this drug has potential side effects, such as thrombocytopenia, an escalation dose regimen was reported to cause an approximately 50% decrease in platelet levels initially, but a similar steady-state effect was induced through the continuous administration of a high dosage (Lock et al., 2008; Shoemaker et al., 2008; Tse et al., 2008). In the present study, when ABT-263 was administered orally to model mice with senescent RPE and retinal degeneration for 7 days, both structural and functional recovery of the retina was observed along with a reduction in senescence phenotypes without overt retinal or systemic toxicity. In addition, the proliferative activity of the RPE was partially recovered in mice treated orally with ABT-263. Therefore, ABT-263 might have the potential to treat AMD by targeting senescent RPE cells. It could be used for combination therapy for wet AMD: periodic oral administration of this drug might reduce the number of anti-VEGF injections needed to treat wet AMD. Moreover, ABT-263 could be developed as the first oral drug for treating dry AMD through the selective elimination of senescent RPE cells, the source of chronic inflammation in the retina responsible for the progression of AMD.

ACKNOWLEDGMENTS

This paper was supported by Konkuk University in 2021.

AUTHOR CONTRIBUTIONS

H.C. conceived and designed the experiments. W.R., C.W.P., H.C., and H.L. wrote the initial draft of the manuscript and analyzed the data. W.R., C.W.P., and J.K. performed the experiments.

CONFLICT OF INTEREST

The authors have no potential conflicts of interest to disclose.

ORCID

Wonseon Ryu https://orcid.org/0000-0001-5604-1803
Chul-Woo Park https://orcid.org/0000-0003-1471-8366
Junghoon Kim https://orcid.org/0000-0002-9517-9087
Hyungwoo Lee https://orcid.org/0000-0002-3248-4754
Hyewon Chung https://orcid.org/0000-0003-1312-6406

REFERENCES

Arepalli, S. and Kaiser, P.K. (2021). Pipeline therapies for neovascular age related macular degeneration. Int. J. Retina Vitreous *7*, 55.

Birch, J. and Gil, J. (2020). Senescence and the SASP: many therapeutic avenues. Genes Dev. *34*, 1565-1576.

Cabral de Guimaraes, T.A., Daich Varela, M., Georgiou, M., and Michaelides, M. (2022). Treatments for dry age-related macular degeneration: therapeutic avenues, clinical trials and future directions. Br. J. Ophthalmol. *106*, 297-304.

Chae, J.B., Jang, H., Son, C., Park, C.W., Choi, H., Jin, S., Lee, H.Y., Lee, H., Ryu, J.H., Kim, N., et al. (2021). Targeting senescent retinal pigment epithelial cells facilitates retinal regeneration in mouse models of age-related macular degeneration. Geroscience *43*, 2809-2833.

Chang, J., Wang, Y., Shao, L., Laberge, R.M., Demaria, M., Campisi, J., Janakiraman, K., Sharpless, N.E., Ding, S., Feng, W., et al. (2016). Clearance of senescent cells by ABT263 rejuvenates aged hematopoietic stem cells in mice. Nat. Med. *22*, 78-83.

Chen, Y., Bedell, M., and Zhang, K. (2010). Age-related macular degeneration: genetic and environmental factors of disease. Mol. Interv. *10*, 271-281.

Childs, B.G., Durik, M., Baker, D.J., and van Deursen, J.M. (2015). Cellular senescence in aging and age-related disease: from mechanisms to therapy. Nat. Med. *21*, 1424-1435.

Comparison of Age-related Macular Degeneration Treatments Trials (CATT) Research Group, Maguire, M.G., Martin, D.F., Ying, G.S., Jaffe, G.J., Daniel, E., Grunwald, J.E., Toth, C.A., Ferris, F.L., 3rd, and Fine, S.L. (2016). Five-year outcomes with anti-vascular endothelial growth factor treatment of neovascular age-related macular degeneration: the comparison of age-related macular degeneration treatments trials. Ophthalmology *123*, 1751-1761.

Cox, J.T., Eliott, D., and Sobrin, L. (2021). Inflammatory complications of intravitreal anti-VEGF injections. J. Clin. Med. *10*, 981.

Crespo-Garcia, S., Tsuruda, P.R., Dejda, A., Ryan, R.D., Fournier, F., Chaney, S.Y., Pilon, F., Dogan, T., Cagnone, G., Patel, P., et al. (2021). Pathological angiogenesis in retinopathy engages cellular senescence and is amenable to therapeutic elimination via BCL-xL inhibition. Cell Metab. *33*, 818-832. e7.

Di Micco, R., Krizhanovsky, V., Baker, D., and d'Adda di Fagagna, F. (2021). Cellular senescence in ageing: from mechanisms to therapeutic

opportunities. Nat. Rev. Mol. Cell Biol. *22*, 75-95.

Ding, X., Patel, M., and Chan, C.C. (2009). Molecular pathology of age-related macular degeneration. Prog. Retin. Eye Res. *28*, 1-18.

Dubik, N. and Mai, S. (2020). Lamin A/C: function in normal and tumor cells. Cancers (Basel) *12*, 3688.

Falavarjani, K.G. and Nguyen, Q.D. (2013). Adverse events and complications associated with intravitreal injection of anti-VEGF agents: a review of literature. Eye (Lond.) *27*, 787-794.

Gandhi, L., Camidge, D.R., Ribeiro de Oliveira, M., Bonomi, P., Gandara, D., Khaira, D., Hann, C.L., McKeegan, E.M., Litvinovich, E., Hemken, P.M., et al. (2011). Phase I study of Navitoclax (ABT-263), a novel Bcl-2 family inhibitor, in patients with small-cell lung cancer and other solid tumors. J. Clin. Oncol. *29*, 909-916.

Han, Z., Liang, J., Li, Y., and He, J. (2019). Drugs and clinical approaches targeting the antiapoptotic protein: a review. Biomed Res. Int. *2019*, 1212369.

Handa, J.T., Bowes Rickman, C., Dick, A.D., Gorin, M.B., Miller, J.W., Toth, C.A., Ueffing, M., Zarbin, M., and Farrer, L.A. (2019). A systems biology approach towards understanding and treating non-neovascular age-related macular degeneration. Nat. Commun. *10*, 3347.

Huang, W., Hickson, L.J., Eirin, A., Kirkland, J.L., and Lerman, L.O. (2022). Cellular senescence: the good, the bad and the unknown. Nat. Rev. Nephrol. *18*, 611-627.

Kim, S. and Kim, C. (2021). Transcriptomic analysis of cellular senescence: one step closer to senescence atlas. Mol. Cells *44*, 136-145.

Kipps, T.J., Eradat, H., Grosicki, S., Catalano, J., Cosolo, W., Dyagil, I.S., Yalamanchili, S., Chai, A., Sahasranaman, S., Punnoose, E., et al. (2015). A phase 2 study of the BH3 mimetic BCL2 inhibitor navitoclax (ABT-263) with or without rituximab, in previously untreated B-cell chronic lymphocytic leukemia. Leuk. Lymphoma *56*, 2826-2833.

Kirkland, J.L. and Tchkonia, T. (2015). Clinical strategies and animal models for developing senolytic agents. Exp. Gerontol. *68*, 19-25.

Kozlowski, M.R. (2012). RPE cell senescence: a key contributor to age-related macular degeneration. Med. Hypotheses *78*, 505-510.

Lee, G. (2022). Cellular senescence: the villain of metabolic disease? Mol. Cells *45*, 531-533.

Lock, R., Carol, H., Houghton, P.J., Morton, C.L., Kolb, E.A., Gorlick, R., Reynolds, C.P., Maris, J.M., Keir, S.T., Wu, J., et al. (2008). Initial testing (stage 1) of the BH3 mimetic ABT-263 by the pediatric preclinical testing program. Pediatr. Blood Cancer *50*, 1181-1189.

Lopez-Otin, C., Blasco, M.A., Partridge, L., Serrano, M., and Kroemer, G. (2013). The hallmarks of aging. Cell *153*, 1194-1217.

Mohamad Anuar, N.N., Nor Hisam, N.S., Liew, S.L., and Ugusman, A. (2020). Clinical review: navitoclax as a pro-apoptotic and anti-fibrotic agent. Front. Pharmacol. *11*, 564108.

Rudin, C.M., Hann, C.L., Garon, E.B., Ribeiro de Oliveira, M., Bonomi, P.D., Camidge, D.R., Chu, Q., Giaccone, G., Khaira, D., Ramalingam, S.S., et al. (2012). Phase II study of single-agent navitoclax (ABT-263) and biomarker correlates in patients with relapsed small cell lung cancer. Clin. Cancer Res. *18*, 3163-3169.

Serrano, M. and Barzilai, N. (2018). Targeting senescence. Nat. Med. *24*, 1092-1094.

Shoemaker, A.R., Mitten, M.J., Adickes, J., Ackler, S., Refici, M., Ferguson, D., Oleksijew, A., O'Connor, J.M., Wang, B., Frost, D.J., et al. (2008). Activity of the Bcl-2 family inhibitor ABT-263 in a panel of small cell lung cancer xenograft models. Clin. Cancer Res. *14*, 3268-3277.

Tse, C., Shoemaker, A.R., Adickes, J., Anderson, M.G., Chen, J., Jin, S., Johnson, E.F., Marsh, K.C., Mitten, M.J., Nimmer, P., et al. (2008). ABT-263: a potent and orally bioavailable Bcl-2 family inhibitor. Cancer Res. *68*, 3421-3428.

de Vos, S., Leonard, J.P., Friedberg, J.W., Zain, J., Dunleavy, K., Humerickhouse, R., Hayslip, J., Pesko, J., and Wilson, W.H. (2021). Safety and efficacy of navitoclax, a BCL-2 and BCL-XL inhibitor, in patients with relapsed or refractory lymphoid malignancies: results from a phase 2a study. Leuk. Lymphoma *62*, 810-818.

Wilson, W.H., Tulpule, A., Levine, A.M., Dunleavy, K., Krivoshik, A.P., Hagey, A.E., Shovlin, M., Gloria, M.A., Greco, R., Xiong, H., et al. (2007). A Phase 1/2a study evaluating the safety, pharmacokinetics, and efficacy of ABT-263 in subjects with refractory or relapsed lymphoid malignancies. Blood *110*, 1371.

Wong, W.L., Su, X., Li, X., Cheung, C.M., Klein, R., Cheng, C.Y., and Wong, T.Y. (2014). Global prevalence of age-related macular degeneration and disease burden projection for 2020 and 2040: a systematic review and meta-analysis. Lancet Glob. Health *2*, e106-e116.